

Research Description

A. Introduction

Proposed instrument: The goal of this project is to enhance and to transform the Knife-Edge Scanning Microscope (KESM) [29, 30, 32], a “one of a kind” microscopy instrument, into a more widely available system for biological research. KESM is capable of sectioning and imaging whole small animal organs at a sub-micrometer resolution. A prototype KESM instrument was constructed, and its capability was successfully demonstrated by scanning diverse biological organs including whole mouse brains (neuronal circuits and vascular networks) [3, 8, 25, 27], octopus brains [5], and the mouse lung (unpublished results) at submicrometer resolution. This project aims to enhance this prototype significantly, and transform it into a robust system that can be replicated and operated with ease by other research groups and industry partners.

Relevant need in biological studies: The proposed instrument addresses at least two major emerging directions in biological research: (1) “omics” and (2) multi-scale modeling. With the tremendous success of genomics in the 1990’s and beyond, biological research is increasingly moving toward various forms of omics. Many such omics research depend on anatomical information (e.g., connectomics, studying the complete wiring diagram in the brain [40, 41]) or whole-organ-wide genomic information (e.g., the whole-brain gene expression data available through the Allen Brain Atlas [23]). Multi-scale modeling has also become a major methodological paradigm in biological research, attested by the formation of the Multi-scale Modeling Consortium, supported by NSF, NIH, DOE, NASA, etc. (recently, a special issue of IEEE Transactions on Biomedical Engineering was dedicated to multiscale modeling and analysis [45]). In many projects in omics and multi-scale modeling, sub-micrometer microscopy data from whole biological organs are essential yet available tools are unable to meet the demand. The available tools are either high-resolution [2, 11, 37] or whole-organ scale [12, 13, 17, 20, 43], but not both. Few approaches exist that address both resolution and coverage such as the Serial Two-Photon Tomography [38] or All-Optical Histology [42], but they are at least an order of magnitude slower than the KESM. KESM is expected to address all three requirements: high-resolution, high-volume, and high-throughput.

Type of development: Type B (bridging from a ‘one of a kind’ prototype to a broadly available instrument).

Nature of improvement: The improvement on the prototype instrument will focus on “broadening accessibility” with enhanced capabilities:

1. Enhanced imaging: (1) higher resolution optics, (2) fluorescence imaging capability, (3) enhanced linescan camera, and (4) improved illumination through the knife.
2. Enhanced mechanical control: (1) more rigid, higher resolution motion stage, and (2) improved motion control algorithms.
3. Enhanced cutting: (1) reduction of cutting artifact through the use of piezoelectric vibrators, and (2) realtime monitoring of cutting-induced vibration (chatter) using accelerometers.
4. Enhanced robustness: (1) realtime imaging error detection and correction, (2) improved pump system for tissue extraction, and (3) enhanced system calibration (focusing and positioning).

The overall resulting improvement can be summarized as follows: (1) 3X improvement in imaging resolution, (2) 10X improvement in robustness of operation, (3) 10X improvement in imaging speed (compared to competing methods [see Table 1]), (4) new fluorescence imaging capability.

Broader impacts: (1) *Impact on the research community:* The enhanced KESM will allow researchers to obtain high resolution, whole-organ data for multiscale investigation of biological organs. (2) *Impact on education:* Microscopic atlases of whole biological organs, such as the web-based KESM mouse brain atlas developed by the project team, can serve as an educational resource for students and educators at all levels (K-12, undergraduate, graduate, and general public). As part of this project, graduate and undergraduate students will be trained in a multidisciplinary environment (neuroscience and computer science). (3) *Instrument dissemination plan:* The project team will collaborate with 3Scan, a start-up company that licensed the KESM patent, to streamline system integration and manufacturing of the KESM instrument for broader dissemination. Technological advances made by the project team will be translated into robust engineering products by 3Scan.

B. Background

In this section, we will provide a brief review of high-throughput imaging methods. Currently, the standard approach for microscopic imaging of a volume of tissue is confocal microscopy [2]. The basic idea is to change the depth of focus (focal plane), and use a pinhole aperture to detect photons originating only from the target depth. This is called “optical sectioning” where virtual, not actual, sections are obtained. In conventional optical sectioning, the main limiting factor is not in the resolution along the x - y plane (~ 250 nm) but in that of the z direction (~ 700 nm) [36]. Although the resolution and imaging depth can be improved using more advanced schemes such as multi-photon microscopy [11], optical sectioning techniques are limited to the tissue surface and have limited z -axis resolution. Slow imaging speed is another issue, for both confocal and multi-photon, such that even in enhanced two-photon microscopy, the data rate is less than 8 MB/s (512×484 at 30 frames/s reported in [14], and about 1 frame/s in [11]).

Physical sectioning combined with microscopy is one alternative to overcome the above issues, since z -axis resolution depends only on how thin the tissue can be sectioned (it can go down to ~ 30 nm using a vibrating microtome), and there is virtually no depth limit on the tissue thickness.

The five most notable approaches in this direction are listed below: (1) All-Optical Histology [42]. (2) Knife-Edge Scanning Microscopy (KESM) [3, 7, 25, 29, 30, 32, 33] (cf. [24]). (3) Serial Two-Photon Tomography [38]. (4) Array Tomography [9, 34]. (5) Serial-Block-Face Scanning Electron Microscopy (SBF-SEM) [10]. (6) Automatic Tape-Collecting Lathe Ultramicrotome (ATLUM) [18, 19]. Table 1 provides a summary comparison of these microscopy methods.

Table 1: Summary Comparison.

Method	High-Resolution	High-Volume	High-Throughput
KESM [25] (cf. [24])	✓	✓	✓
All-Optical Hist. [42]	✓	✓	—
Serial Two-Photon Tomography [38]	✓	✓	—
Array Tomography [35]	✓	—	—
SBF-SEM [10]	✓	—	—
ATLUM [19]	✓	✓	—
MRI/diffusion MRI [17, 20]	—	✓	✓
High-resolution: < 1 μm (diameter of dendrites, axons, capillaries, etc.); High-Volume: > 1 cm^3 (approximate volume of mouse brain and other organs); High-Throughput: < 100 hours (for ~ 50 scanned organs per year).			

Even though the methods above are unified under the common theme of physical sectioning, the resolution and the typical volume they can handle all differ, putting them in a relatively complementary role with respect to each other. In other words, these methods cannot be ranked on an absolute scale since there are relative advantages and disadvantages to each method.

C. Prior Work

C.1. Knife-Edge Scanning Microscope

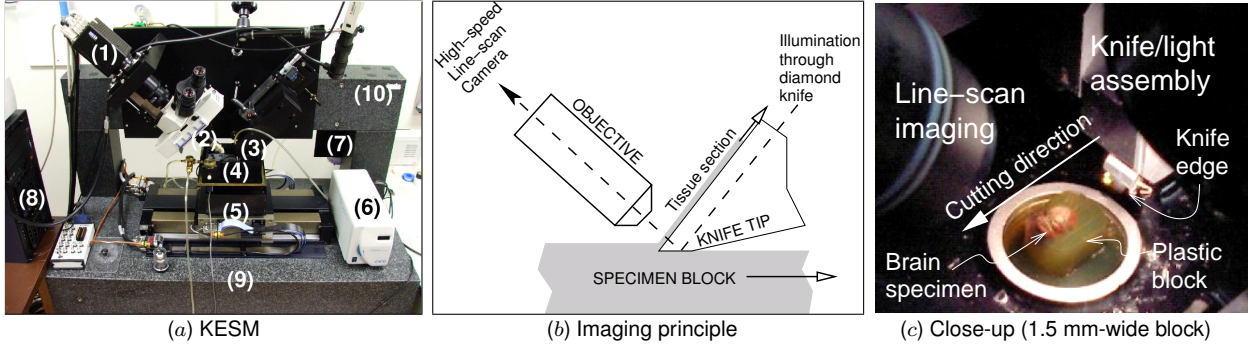


Figure 1: The Knife-Edge Scanning Microscope (KESM 1.0). (a) Photo of the KESM 1.0 instrument showing (1) high-speed line-scan camera, (2) microscope objective, (3) diamond knife assembly and light collimator, (4) specimen tank (for water immersion imaging), (5) three-axis precision air-bearing stage, (6) white-light microscope illuminator, (7) water pump (in the back) for the removal of sectioned tissue, (8) PC server for stage control and image acquisition, (9) granite base, and (10) granite bridge. (b) Specimen undergoing sectioning by knife-edge scanner (thickness of section is not drawn to scale). (c) Close-up photo of the line-scan/microscope assembly and the knife/illumination (knife and objective raised to show the brain specimen).

A prototype Knife-Edge Scanning Microscope (KESM, US patent #6,744,572) [29, 30, 33] has been designed at Texas A&M University (TAMU) with support from the National Science Foundation (MRI award #0079874; McCormick, PI), the Texas Higher Education Coordinating Board (ATP award #000512-0146-2001; Keyser, PI), and the National Institute of Neurological Disorders and Stroke (Award #1R01-NS54252; Choe, PI). The instrument, shown in Fig. 1a, is capable of scanning a complete mouse brain ($\sim 310 \text{ mm}^3$) at 300 nm sampling resolution within 100 hours when scanning in full production mode. The instrument comprises four major subsystems: (1) precision positioning stage, (2) microscope/knife assembly, (3) image capture system, and (4) cluster computer. The specimen, a whole mouse brain, is embedded in a plastic block and mounted atop a three-axis precision positioning stage. A custom diamond knife, rigidly mounted to a massive granite bridge overhanging the three-axis stage, cuts consecutive thin sections from the block. Unlike block face scanning, the KESM concurrently cuts and images (under water) the tissue ribbon as it advances over the leading edge of the diamond knife. A white light source illuminates the rear of the diamond knife, and in turn illuminates the brain tissue at its leading edge, with a strip of intense illumination reflected from the beveled knife-edge, as illustrated in Fig. 1b. Thus, the diamond knife performs two distinct functions: as an optical prism in the collimation system, and as the tool for physically cutting the thin serial sections. The microscope objective, aligned perpendicular to the top facet of the knife, images the transmitted light. A high-sensitivity line-scan camera repeatedly samples the newly cut section, imaging a stripe 20 μm -long along the cutting direction on the tissue ribbon and just beyond the knife-edge, prior to subsequent deformation of the tissue ribbon after imaging. Finally, the digital video signal is passed through image acquisition

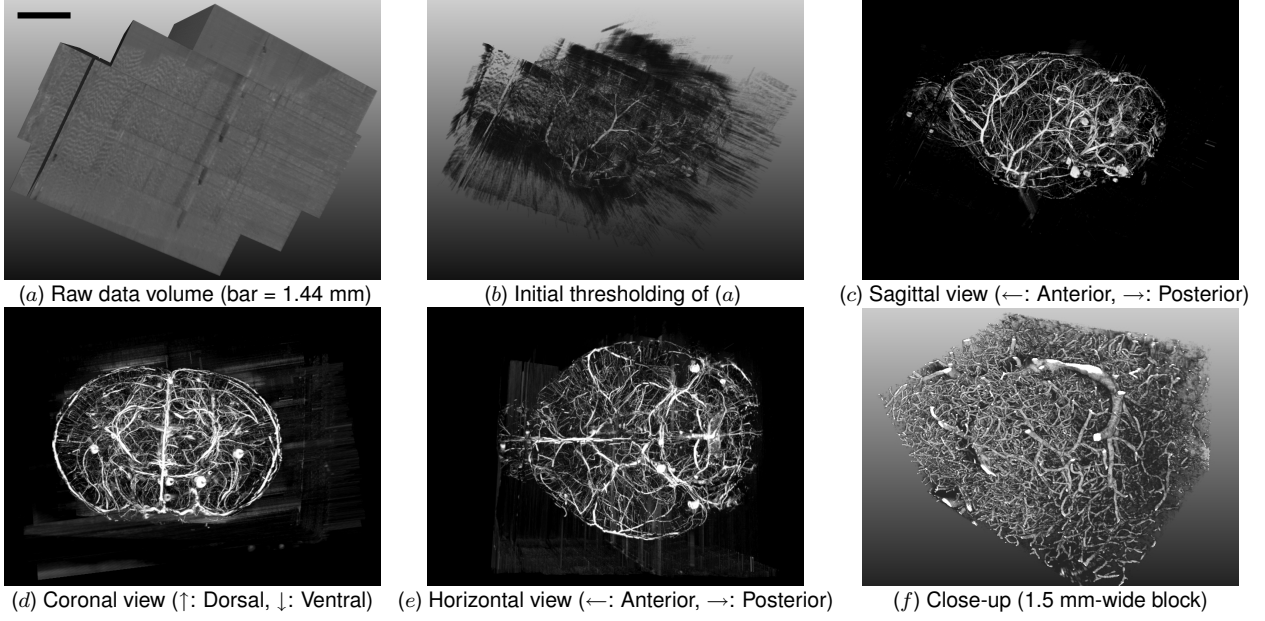


Figure 2: KESM Vasculature Data. Various views of the whole-brain KESM vasculature data are shown. (a) shows the raw data block in a sagittal view (scale bar = 1.44 mm). Note that there are 5 tilted columns, with the top of each column facing the upper-left corner of the figure. (b) shows a slightly thresholded version of (a) so that the boundary of the raw data block and the content within can be seen at the same time. (c) is a fully thresholded version of (a) and (b). (d)–(e) show the coronal and horizontal views, respectively. We can clearly see the shape of the brain. (f) shows the intricate details within an 1.5 mm-wide block.

boards and stored in a dedicated cluster computing system.

C.2. Imaging results of neurons and neurovasculature using KESM

The prototype KESM has been validated on Golgi-, Nissl-, and India-ink-stained mouse brain specimens, and is currently producing high-quality 2D and 3D data. Our pilot results also include data from Golgi-stained octopus optic lobe and subesophageal mass [5]. *India ink* stains all blood vessels in the tissue sample. Major arteries and veins down to the smallest capillaries are stained, revealing a complex network (Fig. 2). *Golgi staining*, in contrast, reveals the entire structure of neurons and, as it stains just 1% of all neurons in the tissue, individual neurons can be seen clearly, permitting reconstruction (Fig. 3). *Nissl staining* dyes the RNA in the cytoplasm of all neurons and the DNA in cell bodies in all cells. However, the dendritic arbors and axons remain unstained. Thus, Nissl staining allows us to reconstruct the distribution of all cell bodies in the mouse brain. Of particular importance is the distribution of cell bodies within the six layers of the cerebral cortex (Fig. 4).

C.3. Results from prior NSF support

For results from the NSF MRI award (#0079874, PI: McCormick), see §C–§C.2. The NSF-supported MRI project received two subsequent funding from the Texas Higher Education Coordinating Board (ATP#000512-0146-2001; Keyser, PI) and the National Institute of Neurological Disorders and Stroke (#1R01-NS54252; Choe, PI), producing over 30 publications since 2001. Co-PI Keyser’s research (#0220047; Keyser, PI) on accurate and robust operations on curved geometry resulted in 12 publications (see CV). The prior support by NSF most immediately relevant to this proposal is the NSF Collaborative Research in Computational Neuroscience Program’s data sharing grant #0905041 (PI: Choe). The main, direct outcome of this grant is the KESM Brain Atlas,

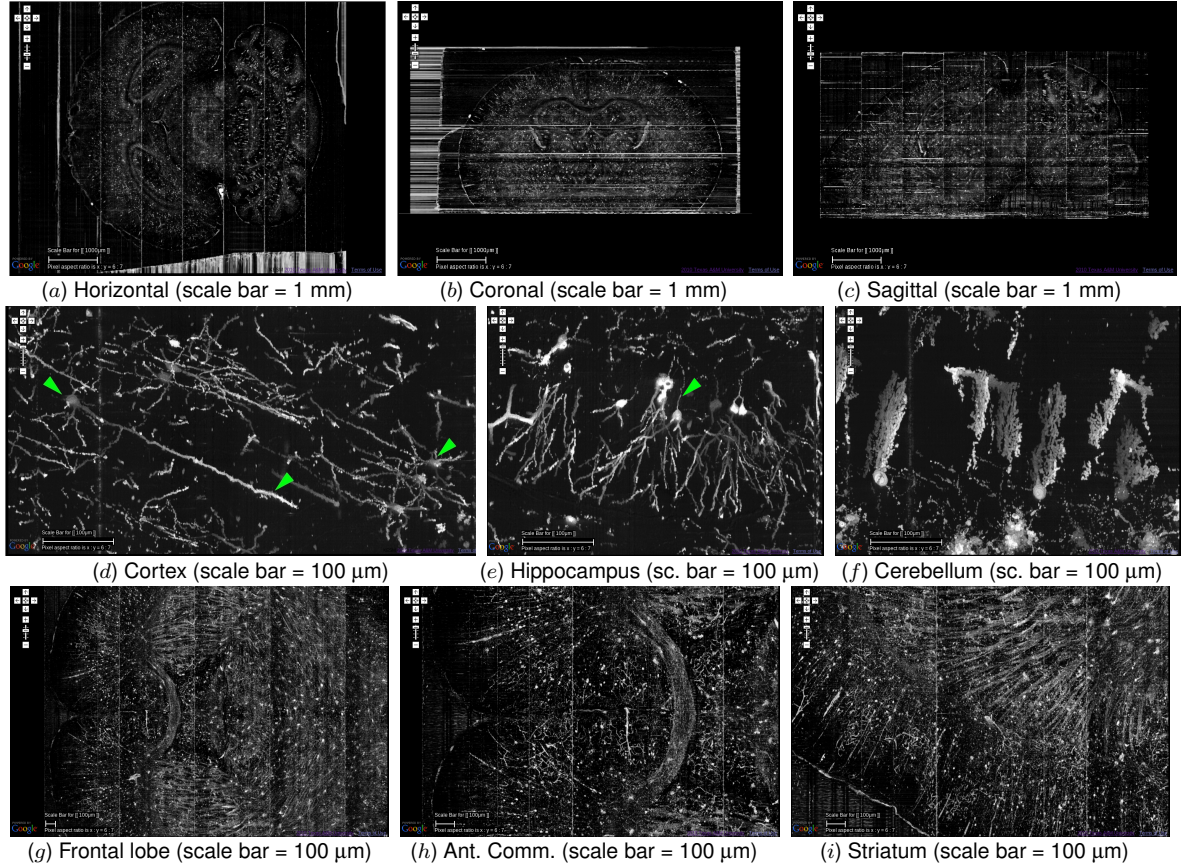


Figure 3: KESM Golgi Data. (a)–(c) Macro-scale views of the KESM Golgi data. (d)–(f) Close-up, showing morphological details of neurons. Arrows (from left to right): pyramidal cell body and apical dendrite. Spiny stellate cells. Hippocampal neuron’s axon. (g)–(i) Mid-scale view showing major fiber pathways.

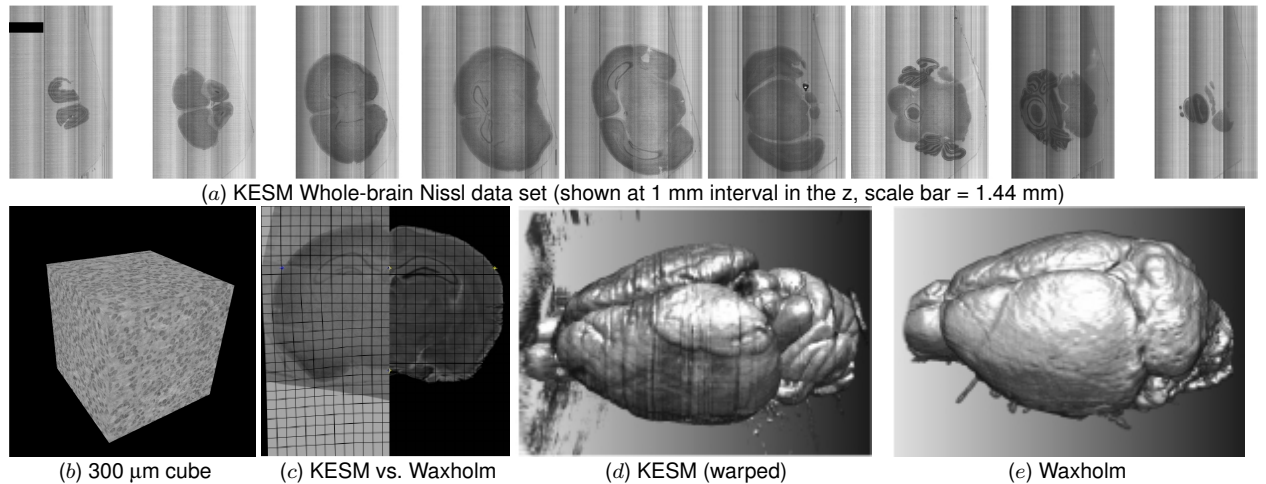


Figure 4: KESM Nissl Data Set. Whole-brain Nissl data set from the KESM is shown. (a) Coronal sections spanning the entire brain, from anterior to posterior, at an interval of 1 mm, are shown. Voxel resolution = $0.6 \mu\text{m} \times 0.7 \mu\text{m} \times 1.0 \mu\text{m}$. Adapted from [4]. (b) A 300 μm cube is shown. This figure shows the 3D-nature of the KESM data set at its full resolution. (c) Registering the KESM Nissl data set (left) to the Waxholm space (right). The grids show the local warping applied. (d) 3D visualization of the KESM Nissl data volume registered to the Waxholm space. Fine details such as the folds in the cerebellum can be seen (such details are not visible in (e)). (e) 3D visualization of the Waxholm reference atlas.

a web-based atlas containing whole-brain-scale Golgi and India ink data sets from the KESM (<http://kesm.org>). Publications resulting from the CRCNS grant are as follows: Conferences [4, 5, 6, 22, 26], Journals [7, 8, 27].

D. Research Plan

KESM has been used to image several large-scale tissue samples. However, large-scale sub-micrometer imaging is useful in several fields beyond neuroscience and therefore KESM is an excellent candidate for commercialization. While other groups have duplicated and validated the technology by performing large-scale imaging [24], this requires extensive knowledge of machining and optics, making the development of in-house systems impractical as it stands. Several steps are required to refine the current prototype for commercialization and easier in-house construction and operation: (1) Minimizing the size, complexity, and cost. (2) Streamlined custom optics to simplify commercial production and to allow fluorescent imaging. (3) Easy and repeatable instrument calibration and configuration. (4) Robust error detection and correction. All of the proposed changes focus on (a) making the KESM more appealing to a broad research base outside of the field of neuroscience for which it was originally designed and (b) making KESM components simple to fabricate and operate, for commercial distribution and in-house fabrication. We propose to build an enhanced KESM system (dubbed KESM 2.0, to disambiguate from the prototype KESM 1.0). Fig. 5 shows the overall design of KESM 2.0, and a partial implementation of the main optics/imaging subsystem.

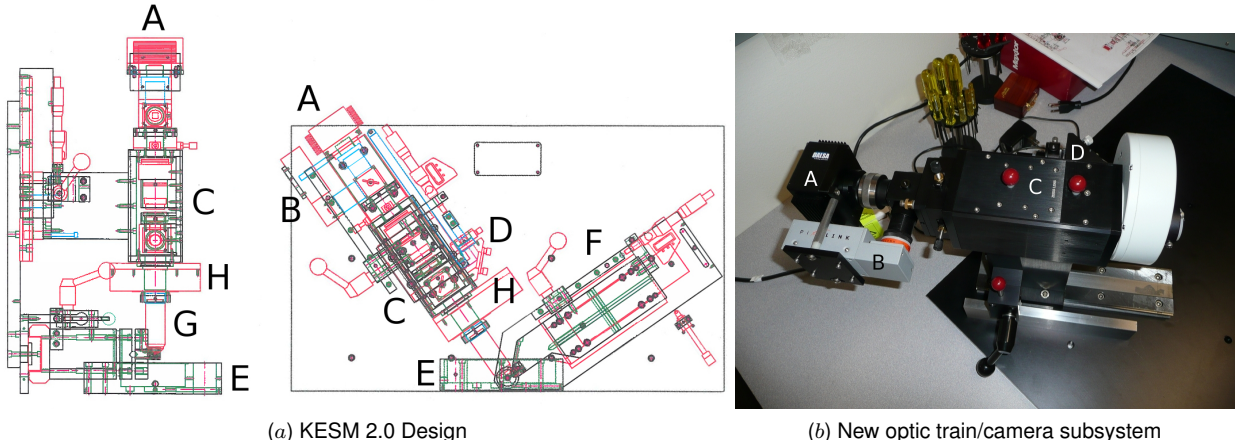


Figure 5: Overview of KESM 2.0 Design and Partial Implementation. (a) The KESM 2.0 design (AutoCAD drawing): side view of optic train/camera (left) and front view of the main subsystems (right). A: main line scan camera, B: auxiliary camera, C: optic train (field lens module), D: laser port for knife alignment and fluorescence illumination, E: specimen tank (stage below the tank is not shown), F: knife mount, G: objective, H: magnification changer. (b) A partial implementation of the design (including the optic train, two new cameras, and laser port for knife orientation calibration: A, B, C, D in (a)). The knife-mount is almost the same as the current KESM, so the initial plan was to reuse the mount from the current KESM. However, to preserve the only working prototype, we will build another replica of the knife mount for use with KESM 2.0.

D.1. Enhanced imaging

1. Higher resolution optics: We have completed the design and construction of a new optical subsystem that allows significantly higher resolution imaging (Fig. 5). This is accomplished through the use of two new objectives: an Olympus 20X 0.95NA objective and a Zeiss 63X 1.0NA

objective (Table 2). The Zeiss 63X allows for the highest resolution, accommodating a field-of-view of 0.317mm and an optimal optical resolution of \sim 168nm. The Olympus 20X objective allows a much larger field-of-view of 1.1mm with a slightly reduced resolution of \sim 177nm. In addition, the Olympus objective allows us to take advantage of advances in camera hardware that allow the full field of view to be imaged at a rate of 68kHz using an 8k line-scan camera. This provides a usable data rate of approximately 450MB/s.

Table 2: Technical Data of the Proposed Objectives for KESM 2.0. See [31] for details.

Optics	Olympus	Carl Zeiss
Objective	XLUMPLFL 20XW	63X PLAN Apochromat (VIS-IR)
Manufacturer's Part #	1-UB965	441470-9900-000
Magnification	10 \times	64 \times
Working distance	2.0 mm	2.1 mm
Numerical Aperture (NA)	0.95	1.0
Access angle	31°(modified to 35°)	35°
Parfocal length	75 mm	45 mm
Focal length	9 mm	2.1 mm
Pupil diameter	12.8 mm	4.2 mm
Field number (FN)	22 mm	20 mm
Changer magnification	1 \times , 1.25 \times , 1.6 \times , 2 \times	Not used (1 \times)
Field of view	1.1 mm at 1 \times mag.	0.317 mm

The constructed collimator assembly is also compatible with multiple objectives, allowing users to purchase objectives that provide a suitable resolution and data rate. Besides the objective, all components of the optical system are now fully customized and can be manufactured by industry collaborators. We must complete one round of testing to validate the new system and make final modifications. We will validate the upgraded system with our mouse brain specimens (Golgi, Nissl, and India ink) and the octopus brain samples (Golgi).

2. Fluorescence imaging: The KESM 2.0 will be adapted to allow imaging of fluorescent tissue. We have performed preliminary evaluation of fluorescence imaging using KESM 1.0 by adapting the optical train to provide excitation illumination through the objective (Fig. 6). These modifications allowed us to successfully image beads perfused with fluorescent polymer and specifically designed to act as a proxy for fluorescent tissue.

However, comparison between fluorescent beads and transgenic zebrafish expressing GFP show a significant drop in emission intensity using the same level of excitation. Therefore the current optical system is not sensitive enough to provide comparable imaging speed for transgenic animals. We propose two modifications to enhance the emission signal for fluorescent tissue: (a) The use of high-intensity coherent excitation and (b) higher sensitivity cameras.

Excitation illumination is currently provided through the diamond knife using a filtered incoherent source. This provides similar illumination intensity to a 25 mW coherent laser. Funding will allow us to upgrade to a 150 mW laser, providing over a 10X increase in excitation energy. We will initially experiment with fluorescence proxies (latex beads), and gradually move to transgenic mouse (GFP expressing in GABAergic neurons) and zebrafish (GFP expressing in Cholinergic neurons). Optimal embedding protocol for large volumes of tissue will be developed to prevent quenching of fluorescence during the embedding process (see [1, 7] for details).

3. Enhanced linescan camera: The current KESM 1.0 detector is a Dalsa CT-F3 line-scan TDI camera with a 180DN/(nJ/cm²) responsivity. We will upgrade to a Dalsa Piranha HS TDI camera, with a responsivity of 1170 DN/(nJ/cm²), providing an \sim 5X increase in sensitivity. This new cam-

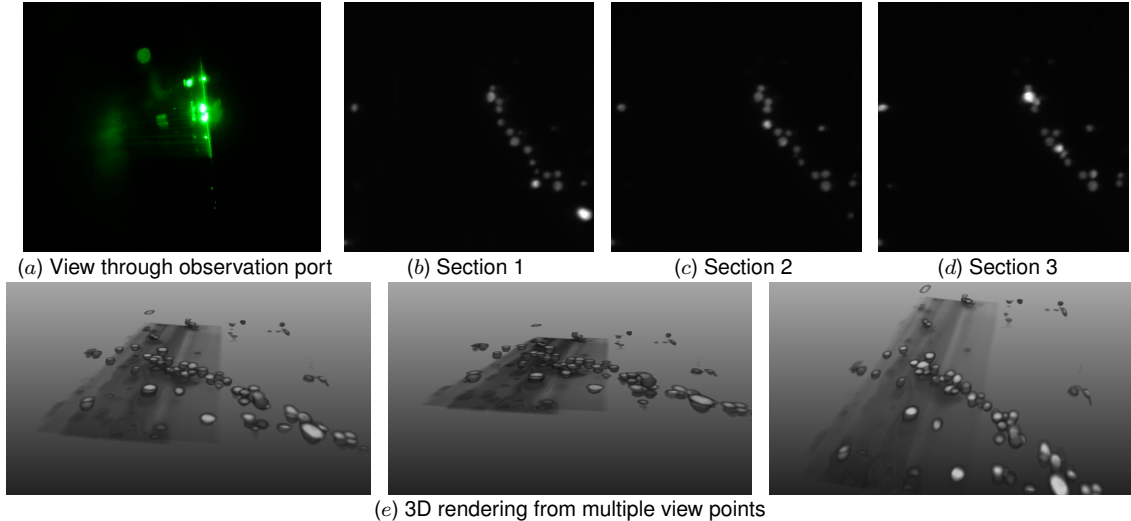


Figure 6: Fluorescence Pilot Results using KESM 1.0. Initial fluorescence imaging results using KESM 1.0 are shown. Latex beads ($10\text{ }\mu\text{m}$ diameter) embedded in nitrocellulose were imaged, using 473 nm, 25 mW diode laser line generator (excitation) and Chroma D535/40M 34320 512 nm–552 nm emission filter. (a) Fluorescence observed through observation port. Scattered latex bead debris can be seen on the knife edge (long vertical bright region in the middle). (b)–(d) Fluorescence scanned with KESM 1.0. The images appear as grayscale since we are using a monochrome linescan camera. (e)–(f) 3D rendering of a small volume including (b)–(d).

era provides a 4X higher data rate for bright-field imaging. Since camera throughput is the current bottleneck in KESM imaging, this will result in a 4X increase in KESM acquisition speed for bright-field, which has already been extensively validated. While we do not expect fluorescence imaging to maintain the same data rate as brightfield, successful validation of fluorescence imaging will result in over a 10X increase in imaging speed and volume size compared to confocal imaging of the same tissue.

4. Improved illumination through the knife: Bright-field illumination in KESM is generally provided in transmission mode through the diamond knife (Fig. 7). While reflection illumination can be provided through the standard microscope light-path, transmission illumination provides better contrast and allows imaging of non-reflective samples (cf. [24] that uses reflection illumination, thus it has a significantly lower data rate compared to the KESM and it cannot image non-reflective stains such as India ink). However, over long periods of imaging, fluctuations in illumination can affect image quality. In particular, intensity fluctuations due to AC voltage oscillations are a common issue in microscopy. These oscillations have a unique impact on KESM imaging, since the high speed of image capture makes these oscillations visible across a single tissue section. In addition, low-frequency oscillations caused by constant lamp usage and variable cutting velocity can change illumination intensity from section to section.

In order to address both of these issues, we propose the use of a completely computer controlled DC illumination source (X-CITE exacte). This provides constant illumination intensity, thereby eliminating the need for post-processing to remove oscillation artifacts. In addition, illumination intensity can be monitored by the imaging system and dynamically adjusted to optimize image quality without user input.

The proposed illumination system uses an X-CITE exacte illuminator and liquid-optic light guide. Successful application of this technology will (1) remove the need for manually adjusted

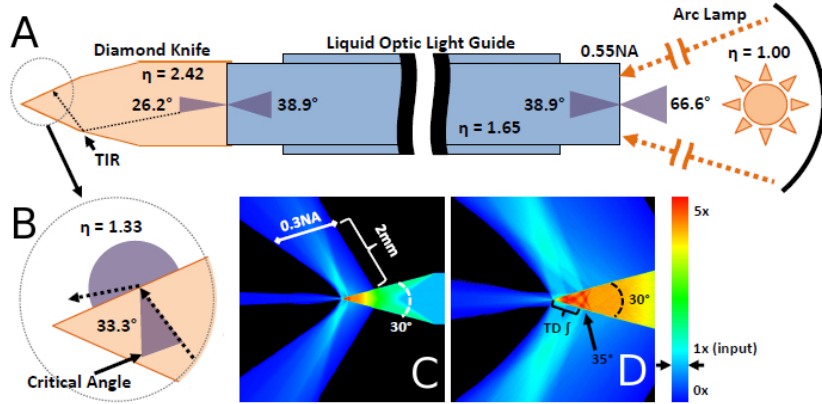


Figure 7: Modeling Illumination Through the Knife. Modeling and analysis of light transmission through the diamond knife is shown. *A*: Geometrical angles of transmitted light waves through the knife and optical properties of the illumination path are shown. *B*: Total internal reflection within the knife results in light scattering and emission through the knife tip. *C–D*: The density of illumination around the knife estimated using a first-order Monte Carlo simulation.

illumination and (2) remove the need for image postprocessing to remove lighting artifacts.

D.2. Enhanced mechanical control

1. More rigid, higher resolution stage: The current KESM prototype positioning mechanics are significantly more cumbersome than necessary for a commercial system. We propose to use the following Aerotech stages: ABL15010-M-10-NC-LN10AS-XYZ-CMS (X Axis), ANT130-110-L-25DU-NONE (Y Axis), AVL125-NC-LTAS (Z Axis). The proposed positioning mechanics reduce the size of the KESM to 1/4 the size of the prototype. The reduction in size also allows significantly higher accuracy and reduced cost. In addition, the proposed controller is implemented completely in software and allows us to control position, image acquisition, and error correction from a single application that can be run remotely. These advances play a crucial role in error detection and correction. We also redesigned the stage mount, to interface better with the rest of the system (Fig. 8a).

2. Improved motion control algorithms: Synchronization between imaging and positioning systems has been validated in the KESM 1.0 prototype, however, a more robust control software will be written to take advantage of the new CameraLink interface and the software-based positioning controller. This integrated software control system is essential to the operation of the KESM 2.0, and is mostly incomplete at the moment. Funding from this project will enable the authoring and refinement of this important module.

D.3. Enhanced cutting

1. Piezo-electric vibrators: The suppression of nonlinear vibration is an active area of research in machining. In particular, knife chatter plays an important role in image quality, particularly at high resolution where the sample rate approaches the frequency of potential vibrations. As sequential sections are cut, knife chatter is often reinforced across multiple sections. Currently, this reinforcing is prevented by adjusting cutting velocity slightly from section to section. However, this introduces complications by (a) introducing an overall reduction in imaging speed and (b) requiring additional processing to adjust image intensity to compensate for a varying exposure time.

We propose to modify the current knife module to include a piezoelectric vibrator that oscillates the knife at high frequency in a direction orthogonal to the cutting direction (Fig. 9). This has been shown to dramatically reduce knife chatter in ultramicrotomes (vibratomes). In addition, piezoelectric oscillators provide an inexpensive means of chatter suppression that may be able to loosen the tight constraints on stiffness imposed on the positioning system and cutting tool (see the modified knife mount adjust plates in Fig. 8b–c).

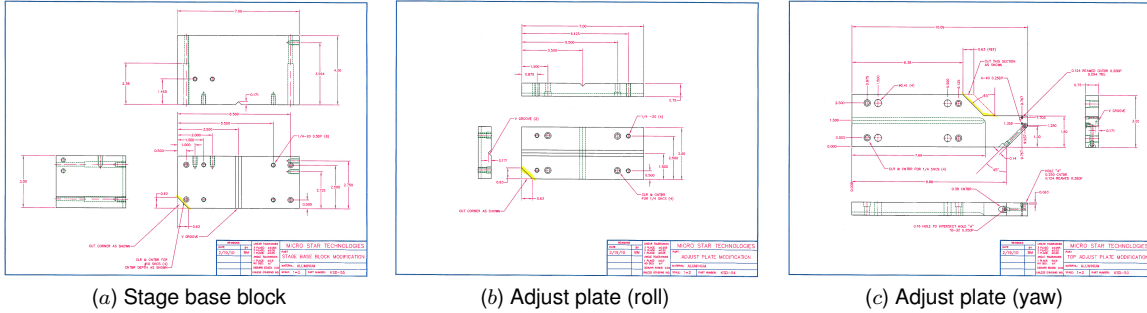


Figure 8: Stage Base and Knife Mount Design for KESM 2.0. CAD drawings of the (a) stage base and (b)–(c) knife mount modifications are shown.



Figure 9: New Knife Module (KESM 2.0). The new knife module design and implementation are shown. (a) Knife module design that incorporates a piezo-electric vibrator (CAD drawing). (b) Implemented knife module. The electric wire with a gold-plated tip connects to a current source to drive the vibrator. (c) Function generator for vibrator input current generation (top) and oscilloscope with accelerometer to measure vibration (bottom).

The proposed modifications have already been added to our knife module design and are relatively simple and inexpensive to manufacture. We will (1) determine the effectiveness of piezoelectric oscillators for chatter suppression, and (2) evaluate the effect of high frequency knife vibration on image quality.

Success will be determined by an improvement in image quality determined quantitatively: (1) reduced amplitude of periodic oscillation along the y-axis in the Fourier domain, and (2) limited (sub-pixel) blurring along the x-axis resulting from knife vibration.

2. Realtime monitoring of cutting-induced vibration: A constant and difficult source of noise in KESM images is cutting-induced vibration (chatter) that causes uneven cut thickness and streaks perpendicular to the cutting direction [46]. We have established a direct correlation between vibration and imaging noise due to chatter [16] (Fig. 10). We will use piezo-electric accelerometers that we used for our study in [16] to constantly monitor chatter, and take corrective actions such as

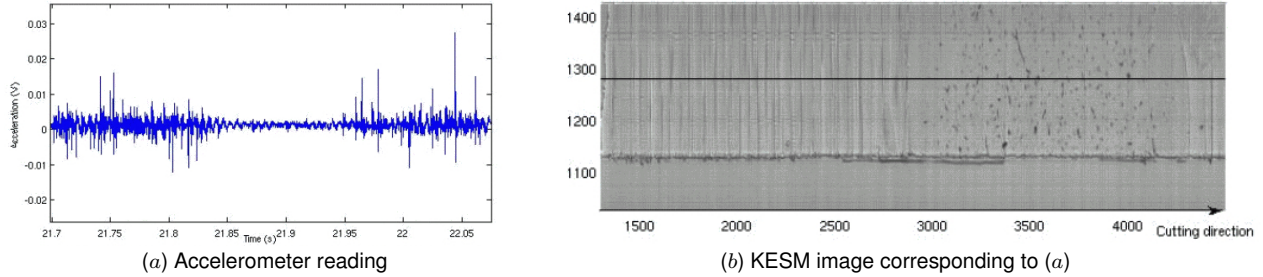


Figure 10: Measuring and Modeling Chatter. (a) Piezo-electric accelerometer reading (top) and the corresponding image acquired from the cutting session (right) are shown. The part with higher acceleration is followed by a lower amplitude region in the middle, again followed by higher amplitude in the acceleration. The lower amplitude region corresponds to the part where actual brain tissue is embedded, while the other regions are plastic only. Pilot result from [16].

dynamically varying the cutting speed within a reasonable range. We found that randomly varying cutting speed can help reduce chatter. We will also investigate cutting characteristics due to variations in the embedding protocol (see [1, 7] for details).

D.4. Enhanced robustness

1. Realtime imaging error detection and correction: Imaging can be interrupted as a result of several malfunctions. Generally, failure of the positioning mechanics does not result in a loss of data. However, malfunctions that occur in illumination, in the optical train, or as the result of a malfunction in the imaging system, can result in continued cutting in the presence of failed acquisition. Since KESM imaging is generally unobserved, and the goal is completely autonomous imaging, error detection and some level of correction must be incorporated in software. Previous experiments indicate that human intervention in the imaging process (in order to find and eliminate errors) every 30 minutes results in a data loss of between 1.0% - 1.5%. The reasons for data loss are often due to (1) stray tissue sections between the knife and objective obstructing imaging, (2) interruptions in illumination, (3) disk malfunction or disk full, and (4) camera faults.

We propose to increase system robustness by implementing error detection as an integral part of the KESM imaging and control software. In several cases, errors can be automatically recovered. Our main improvement is the observation camera (Pixilink IEEE 1394 camera) that shares the light path with the main linescan camera. Routine errors such as obstruction of the view by debris (uncleared tissue ribbon, etc.) can be easily detected with this observation camera. In the case of camera faults, more robust control software is required to detect and reset the imaging device. Interruptions and variations in light intensity will be dynamically controlled using the proposed computer controlled illumination system (X-CITE exacte).

Successful implementation of error detection and correction will be determined by achieving below 0.1% data loss and an average of less than one system halt per 20-hour fully-autonomous imaging period.

2. Improved pump system for tissue extraction: We will improve the tissue extraction mechanism by improving the flow from the knife tip to the pump, and utilizing relay-controlled pump purge system that can reverse the flow of water across the knife tip and remove obstructing debris. Combined with the observation camera discussed right above, tissue obstructions can be cleared easily and only when necessary. For un-recoverable errors, the software will immediately stop sectioning in order to avoid data loss and alert the human operator.

3. Enhanced system calibration (focusing and positioning): The current KESM 1.0 system, although robust, is very difficult to adjust the various mechanical controls for optimal imaging. Stopping and resuming imaging often involves raising the objective and the knife mount so that the stage can freely move and recalibrate. Everytime the objective and knife mount are raised and lowered, there is a slight change in the position of these subsystems relative to each other and to the stage. This results in slight translation of the imaging location. Furthermore, getting the knife aligned parallel to the imaging plane is very difficult. All of the above, combined with the camera position adjustment controls, make focusing a very difficult task that requires extreme expertise. This kind of expertise is unacceptable for a highly available and widely used instrument. We propose to introduce fundamental changes to the system to make focusing and positioning much easier.

The newly introduced observation camera serves a dual purpose. The first is to detect tissue obstruction as mentioned above in this section. The second is to aid in focusing the optic train. Since our new design makes the observation camera and the linescan camera share the same light path, focusing with the observation camera will automatically focus the linescan camera (Fig. 11a). The new laser port also serves a dual purpose. It will be used for fluorescence illumination, and for calibrating the knife orientation. The frosted glass in the laser port will be used to align the laser input and the laser reflected from the knife (Fig. 11b).

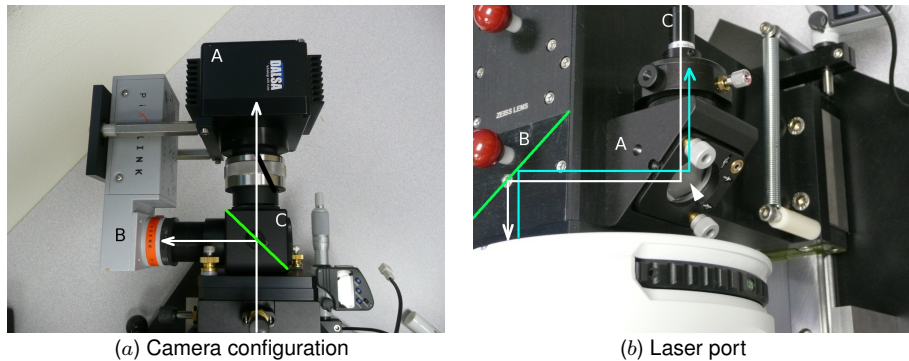


Figure 11: Camera Configuration and Laser Port (KESM 2.0). The camera configuration and laser port are shown. These features enhance robustness of KESM 2.0. (a) The main linescan camera A and the observation camera B share the same light path, with the majority of light going to A at the beam splitter C. (b) The frosted glass (arrowhead) in the laser port A (Fig. 5b, component D) allows laser C to shoot at the knife through the objective (white light path) and observe the reflection (cyan light path) to help align the knife. B is a beam splitter.

Summary: Table 3 summarizes an overall comparison of KESM 1.0 and KESM 2.0.

E. Target Research Community

The target community of our proposed instrument can be categorized as follows. The list includes collaborators (indicated by *, to whom we provided [or plan to provide] pilot data from the KESM) and those who have shown interest in KESM. (1) researchers in our immediate research group (PI, Co-PIs, and graduate students [mouse and rat brain]), (2) on-campus academic collaborators (Thierry Lints [zebra finch]; Michael Smotherman [bats]; Jane Welsh [demyelination]*), (3) off-campus academic collaborators (Stephen J. Smith, Stanford [zebra fish, array tomography]*; George Karniadakis, Brown University [vascular network]; David Edelman, The Neurosciences Institute, San Diego, CA [octopus]*; Graziano Fiorito, Stazion Zoologica Anton Dohrn, Naples, Italy

Table 3: Summary Comparison of KESM 1.0 and KESM 2.0.

	KESM 1.0	KESM 2.0	
Optics			
Optical Train	Nikon Fluorescence Microscope	Custom	
Objectives	Nikon 10X 0.3NA Nikon 40X 0.8NA	Olympus 20X 0.95NA Zeiss 63X 1.0NA	
Illumination			
Bright field Power Voltage Source Computer Controlled	X-CITE 120 120W AC No	X-CITE exacte 200W DC Yes	
Fluorescence	475 nm 25 mW diode laser (experimental)	475 nm 150 mW diode laser	
Camera			
Model Samples Data Rate Light Responsivity	Dalsa CT-F3 4096 133 MB/s 180 DN/(nJ/cm ²)	Dalsa Piranha 8k HS 8192 450 MB/s 1170 DN/(nJ/cm ²)	
Positioning Mechanics			
X-Axis Z-Axis	Size (max length) Accuracy	Aerotech ABL20120 1574 mm Aerotech ANT120 +/- 1 μm	Aerotech ABL 15005 350 mm Aerotech ANT-130-5-V-PLUS +/- 0.2 μm

[octopus]*; Sachiko Koyama, Indiana University [Cholinergic neurons in mouse olfactory system]*; Ching-Long Lin, University of Iowa [mouse lung]*; Gro Amdam, Arizona State University [honey bee brain]*) (4) industrial collaborators (Todd Huffman*, 3Scan; A. Ravi Rao, IBM; Randal Koene, Halcyon Molecular*), (5) general neuroscience community (large number of correspondences at the Society for Neuroscience meeting and the Computational Neuroscience meeting where we organized symposia, workshops, demos, and exhibits), and (6) neuroscience education community.

As the list above shows, KESM is applicable to multiple organs and systems (brain, lung, and vascular system) and diverse biological species (mouse, rat, octopus, zebra fish, zebra finch, bat, and honey bee).

In the following, we will discuss in more detail some representative research projects enabled by the KESM, beyond the mouse brain project currently conducted by the project team. Figure 12 shows pilot results relating to these example projects. (Also see the letters of support.)

1. Mouse lung modeling and computational fluid dynamics simulation (Collaborator: Ching-Long Lin, University of Iowa) For an accurate quantitative modeling of the lung, exact geometric reconstructions of the various airways and microstructures such as acini are necessary. Figure 12a shows a small volume of the mouse lung imaged using the KESM. Data like these, together with computational fluid dynamics algorithms developed at the University of Iowa by Ching-Long Lin's team, can help us understand how the diffusion of gas (and other micro particles) can be controlled through the interaction of the macro- and microstructures in the lung. Individual variations in structure in the lung can also be compared and their effects on the efficiency of the organ can be measured.

2. Octopus connectome project (Collaborator: David Edelman, Neurosciences Institute and Bennington College) The common octopus, *Octopus vulgaris*, is one of the most intelligent invertebrate [15]. Although the organization of the nervous system of the octopus is quite alien

compared to that of the mammal (or any vertebrate) [47], the complex cognitive behavior exhibited by the animal shows striking convergence to that of the mammal [15]. A comparative study of the connectome of the octopus (Golgi preparation) and that of a model mammal such as a mouse can lead to deeper insights into a common set of mechanisms that give rise to intelligent behavior [5]. See Figure 12b–c for pilot results.

3. Neuron-vasculature interaction and demyelination (Collaborator: Jane Welsh, Texas A&M University) The vascular network and neurons in the brain are engaged in a complex interaction. For example, viruses such as Theiler's virus can induce demyelination of axons [44], which is believed to be preceded by the break-down of the blood-brain barrier. A whole-brain-level study of the vascular network and their surrounding neuronal populations (figure 12d–e) prior to and after viral infection can help elucidate the extent of structural interactions among these constituents.

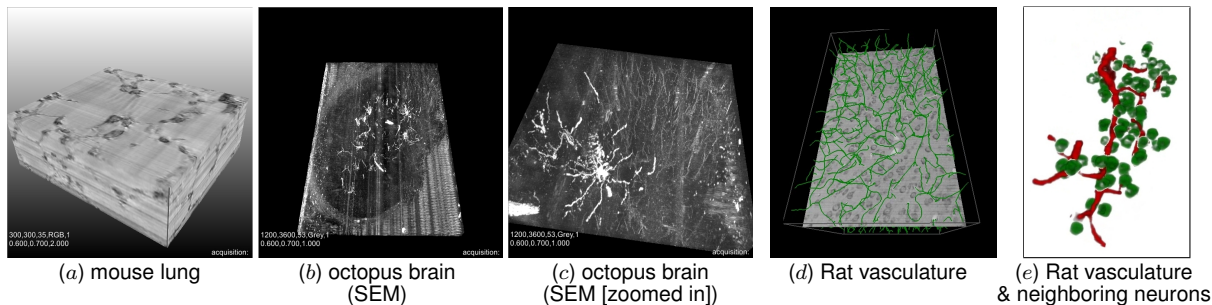


Figure 12: Example Projects. Pilot scans using the KESM are shown to highlight the broad applicability of the instrument to a wide range of biological research. (a) Alveoli in the mouse lung (210 μm -wide block). (b–c) Octopus brain (supraesophageal mass [SEM]). The block widths are 840 μm and 420 μm , respectively. (d–e) Rat brain (somatosensory cortex) vasculature and neighboring neurons (from Nissl data). In (d), dark gray spots are cell nuclei and the white discs are the cross sections of the vascular network (traced in green). In (e), traced vasculature (red) and neighboring neuronal cell bodies (green) are shown.

F. Dissemination Plan

For research groups willing to construct the KESM on their own, we will publish a series of detailed technical reports about KESM 2.0 (see Table 4 for the timeline): (1) Specimen preparation manual. (2) Technical spec (including CAD drawings) and assembly manual for instrument fabrication. (3) Operation manual and best practices. See our earlier tech reports for KESM 1.0 [28] and KESM 1.5 [31], and our detailed specimen preparation and KESM 1.0 operation protocol reported in the Journal of Visualized Experiments [7]. The article includes a 10-minute video tutorial and a detailed protocol document.

For those who need access to a completely integrated system, we will coordinate with 3Scan, a start-up company that is building a robust, commercial version of the KESM. Engineers at 3Scan have been collaborating with the project team in experimental modifications to the KESM system. We will assist 3Scan in acquiring SBIR grants, and we will utilize the STTR and GOALI mechanism to transfer our core technology to 3Scan, for rapid and affordable dissemination.

G. Broader Impact Plan

Student training and under-represented groups: This project will support the training of two Ph.D. students. Our team's previous work in this area also has a strong history of involvement of Master's-level students (not directly funded; seven M.S. theses have come from the group)

and undergraduate students (PIs Keyser and Choe have supervised fourteen undergraduates in the past eight years) under the Research Experience for Undergraduates (REU) program (REU site, #0353957; PI: V. E. Taylor), and the Computing Research Association(CRA)'s Distributed Research Experiences for Undergraduates (DREU) that targets under-represented groups in CS. We will continue our effort in this direction. Our past efforts have demonstrated that we are able to incorporate under-represented groups in the project, including women (currently two of our graduate students are female, and two women have recently graduated) and minority students (primarily at the undergraduate level). We will continue to involve and provide outreach to these groups in our proposed project.

K-12 and public outreach: The resulting new instrument and data, together with the neuroinformatics platform we are developing as part of a separate grant (NSF CRCNS), will also give us an opportunity to reach out to K-12 students and the public alike. PIs Keyser and Choe have had significant experience in interactions with high-school-level groups (such as lab tours) and we will continue these activities. We will set up an educational web site about the KESM project and organize mini-workshops for high school science teachers so that they can utilize our resources in their curriculum. We have also actively collaborated with documentary film projects [21], popular science book projects [39] and TV programs on brain science, and we will continue these activities (a current project on the table is a planned appearance in a History Channel show).

H. Management Plan

Task responsibilities and the time line of the project are shown in Table 4. Directly relevant sections in the research plan are indicated next to each task (as "D.x"). The project team will meet on a weekly basis to discuss issues and progress. By the end of each semester, a small workshop will be organized to sum up and evaluate the semester's work and plan ahead.

Table 4: Tasks and Timeline

Phase	Task	Year 1	Year 2	Responsibility
1. Design and prep.	1.1 System design refinement	■		Choe
	1.2 Parts acquisition	■		Choe
2. Construction	2.1 Knife module (incl. piezo): D.3	■		Choe
	2.2 Knife mount: D.3	■		Choe
3. Software subsys.	2.3 System integration (incl. optics)	■■■		Choe
	3.1 Stage control: D.2	■■■		Choe
4. Robustness	3.2 Imaging: D.1, D.4	■■■		Keyser
	4.1 Vibration monitoring: D.3	■■		Keyser,Abbott
	4.2 Imaging error detection: D.4	■■		Keyser
	4.3 Pump system: D.4	■■■		Choe
5. Testing	4.4 Calibration (focusing/positioning): D.4	■■■		Keyser
	5.1 Specimen preparation	■■■		Abbott
	5.2 Pilot scans (brightfield): D.1		■■■	Abbott,Choe
	5.3 Pilot scans (fluorescence): D.1		■■■	Choe,Abbott
6. Dissemination	5.4 Production scans		■■■	Choe,Abbott
	6.1 Specimen prep. manual		■■■	Abbott
	6.2 Technical documentation		■■■	Choe,Keyser
	6.3 Operations manual		■■■	Choe
	6.4 CAD files		■■■	Keyser,Choe
	6.5 Pathway to mass production		■■■	Choe

REFERENCES CITED

- [1] Abbott, L. C., and Sotelo, C. (2000). Ultrastructural analysis of catecholaminergic innervation in weaver and normal mouse cerebellar cortices. *Journal of Comparative Neurology*, 426:316–329.
- [2] Carlsson, K., Danielsson, P., Lenz, R., Liljeborg, A., and Åslund, N. (1985). Three-dimensional microscopy using a confocal laser scanning microscope. *Optics Letter*, 10:53–55.
- [3] Choe, Y., Abbott, L. C., Han, D., Huang, P.-S., Keyser, J., Kwon, J., Mayerich, D., Melek, Z., and McCormick, B. H. (2008). Knife-edge scanning microscopy: High-throughput imaging and analysis of massive volumes of biological microstructures. In Rao, A. R., and Cecchi, G., editors, *High-Throughput Image Reconstruction and Analysis: Intelligent Microscopy Applications*, 11–37. Boston, MA: Artech House.
- [4] Choe, Y., Abbott, L. C., Miller, D. E., Han, D., Yang, H.-F., Chung, J. R., Sung, C., Mayerich, D., Kwon, J., Micheva, K., and Smith, S. J. (2010). Multiscale imaging, analysis, and integration of mouse brain networks. In *Neuroscience Meeting Planner, San Diego, CA: Society for Neuroscience*. Program No. 516.3. Online.
- [5] Choe, Y., Abbott, L. C., Ponte, G., Keyser, J., Kwon, J., Mayerich, D., Miller, D., Han, D., Grimaldi, A. M., Fiorito, G., Edelman, D. B., and McKinstry, J. L. (2010). Charting out the octopus connectome at submicron resolution using the knife-edge scanning microscope. *BMC Neuroscience*, 11(Suppl 1):P136. Nineteenth Annual Computational Neuroscience Meeting: CNS*2010.
- [6] Choe, Y., Mayerich, D., Kwon, J., Miller, D. E., Chung, J. R., Sung, C., Keyser, J., and Abbott, L. C. (2011). Knife-edge scanning microscopy for connectomics research. In *Proceedings of the International Joint Conference on Neural Networks*, 2258–2265. Piscataway, NJ: IEEE Press.
- [7] Choe, Y., Mayerich, D., Kwon, J., Miller, D. E., Sung, C., Chung, J. R., Huffman, T., Keyser, J., and Abbott, L. C. (2011). Specimen preparation, imaging, and analysis protocols for knife-edge scanning microscopy. *Journal of Visualized Experiments*, 58:e3248. Doi: 10.3791/3248.
- [8] Chung, J. R., Sung, C., Mayerich, D., Kwon, J., Miller, D. E., Huffman, T., Abbott, L. C., Keyser, J., and Choe, Y. (2011). Multiscale exploration of mouse brain microstructures using the knife-edge scanning microscope brain atlas. *Frontiers in Neuroinformatics*, 5:29.
- [9] Datwani, A., McConnell, M. J., Kanold, P. O., Micheva, K. D., Busse, B., Shamloo, M., Smith, S. J., and Shatz, C. J. (2009). Classical MHCI molecules regulate retinogeniculate refinement and limit ocular dominance plasticity. *Neuron*, 64:463–470.
- [10] Denk, W., and Horstmann, H. (2004). Serial block-face scanning electron microscopy to reconstruct three-dimensional tissue nanostructure. *PLoS Biology*, 19:e329.
- [11] Denk, W., Strickler, J. H., and Webb, W. W. (1990). Two-photon laser scanning fluorescence microscopy. *Science*, 248:73–76.

- [12] Duvernoy, H. (1991). *The Human Brain: Structure, Three-Dimensional Sectional Anatomy and MRI*. New York, NY: Springer-Verlag.
- [13] Duvernoy, H. M. (1999). *The Human Brain: Surface, Three-Dimensional Sectional Anatomy With MRI, and Blood Supply*. Newyork, NY: Springer-Verlag. Second edition.
- [14] Fan, G. Y., Fujisaki, H., Miyawaki, A., Tsay, R.-K., Tsien, R. Y., and Elisman, M. H. (1999). Video-rate scanning two-photon excitation fluorescence microscopy and ratio imaging with cameleons. *Biophysical Journal*, 76:2412–2420.
- [15] Fiorito, G., and Scotto, P. (1992). Observational learning in Octopus vulgaris. *Science*, 256:545–547.
- [16] Guntupalli, J. S. (2007). *Physical Sectioning in 3D Biological Microscopy*. Master's thesis, Department of Computer Science, Texas A&M University.
- [17] Hagmann, P., Kurant, M., Gigandet, X., Thiran, P., Wedeen, V. J., Meuli, R., and Thiran, J.-P. (2007). Mapping human whole-brain structural networks with diffusion MRI. *PLoS ONE*, 2:e597.
- [18] Hayworth, K. (2008). Automated creation and SEM imaging of Ultrathin Section Libraries: Tools for large volume neural circuit reconstruction. In *Society for Neuroscience Abstracts*. Washington, DC: Society for Neuroscience. Program No. 504.4.
- [19] Hayworth, K., and Lichtman, J. W. Automatic Tape-Collecting Lathe Ultramicrotome (ATLUM), http://www.mcb.harvard.edu/lichtman/ATLUM/ATLUM_web.htm.
- [20] Jacobs, R. E., Ahrens, E. T., Dickinson, M. E., and Laidlaw, D. (1999). Towards a microMRI atlas of mouse development. *Computerized Medical Imaging and Graphics*, 23:15–24.
- [21] Kurzweil, R., The singularity is near. 2010 Film. <http://www.singularity.com/themovie/>.
- [22] Kwon, J., Mayerich, D., and Choe, Y. (2011). Automated cropping and artifact removal for knife-edge scanning microscopy. In *Proceedings of the IEEE International Symposium on Biomedical Imaging*, 1366–1369.
- [23] Lein et al., E. S. (2007). Genome-wide atlas of gene expression in the adult mouse brain. *Nature*, 445:168–176.
- [24] Li, A., Gong, H., Zhang, B., Wang, Q., Yan, C., Wu, J., Liu, Q., Zeng, S., and Luo, Q. (2010). Micro-optical sectioning tomography to obtain a high-resolution atlas of the mouse brain. *Science*, 330:1404–1408. See the E-Letter commentary by Mayerich et al.
- [25] Mayerich, D., Abbott, L. C., and McCormick, B. H. (2008). Knife-edge scanning microscopy for imaging and reconstruction of three-dimensional anatomical structures of the mouse brain. *Journal of Microscopy*, 231:134–143.
- [26] Mayerich, D., Kwon, J., Panchal, A., Keyser, J., and Choe, Y. (2011). Fast cell detection in high-throughput imagery using gpu-accelerated machine learning. In *Proceedings of the IEEE International Symposium on Biomedical Imaging*, 719–723.

- [27] Mayerich, D., Kwon, J., Sung, C., Abbott, L. C., Keyser, J., and Choe, Y. (2011). Fast macro-scale transmission imaging of microvascular networks using KESM. *Biomedical Optics Express*, 2:2888–2896.
- [28] McCormick, B. H. (2002). Development of the brain tissue scanner. Technical report, Department of Computer Science, Texas A&M University.
- [29] McCormick, B. H. (2003). The knife-edge scanning microscope. Technical report, Department of Computer Science, Texas A&M University. <http://research.cs.tamu.edu/bnl/>.
- [30] McCormick, B. H., System and method for imaging an object. USPTO patent #US 6,744,572 (for Knife-Edge Scanning; 13 claims).
- [31] McCormick, B. H. (2006). KESM 1.5 optics and camera. Technical report, Department of Computer Science, Texas A&M University. <http://research.cs.tamu.edu/bnl/>.
- [32] McCormick, B. H., Abbott, L. C., Mayerich, D. M., , Keyser, J., Kwon, J., Melek, Z., and Choe, Y. (2006). Full-scale submicron neuroanatomy of the mouse brain. In *Society for Neuroscience Abstracts*. Washington, DC: Society for Neuroscience. Program No. 694.5. Online.
- [33] McCormick, B. H., and Mayerich, D. M. (2004). Three-dimensional imaging using Knife-Edge Scanning Microscope. *Microscopy and Microanalysis*, 10 (Suppl. 2):1466–1467.
- [34] Micheva, K., and Smith, S. J. (2007). Array tomography: A new tool for imaging the molecular architecture and ultrastructure of neural circuits. *Neuron*, 55:25–36.
- [35] Micheva, K., and Smith, S. J. (2007). Array tomography: A new tool for imaging the molecular architecture and ultrastructure of neural circuits. *Neuron*, 55:25–36.
- [36] Pawley, J. B. (1995). *Handbook of Biological Confocal Microscopy*. New York: Plenum Press.
- [37] Pawley, J. B. (2005). *Handbook of Biological Confocal Microscopy*. New York: Springer.
- [38] Ragan, T., Kadiri, L. R., Venkataraju, K. U., Bahlmann, K., Sutin, J., Taranda, J., Arganda-Carreras, I., Kim, Y., Seung, H. S., and Osten, P. (2012). Serial two-photon tomography for automated *ex vivo* mouse brain imaging. *Nature Methods*, 9:255–258.
- [39] Schoonover, C. (2010). *Portraits of the Mind: Visualizing the Brain from Antiquity to the 21st Century*. New York, NY: Abrams.
- [40] Seung, H. S. (2012). *Connectome: How the Brain's Wiring Makes Us Who We Are*. Boston, MA: Houghton Mifflin Harcourt.
- [41] Sporns, O., Tononi, G., and Kötter, R. (2005). The human connectome: A structural description of the human brain. *PLoS Computational Biology*, 1:e42.
- [42] Tsai, P. S., Friedman, B., Ifarraguerri, A. I., Thompson, B. D., Lev-Ram, V., Schaffer, C. B., Xiong, Q., Tsien, R. Y., Squier, J. A., and Kleinfeld, D. (2003). All-optical histology using ultrashort laser pulses. *Neuron*, 39:27–41.
- [43] Tuch, D. S., Reese, T. G., Wiegell, M. R., and Wedeen, V. J. (2003). Diffusion MRI of complex neural architecture. *Neuro*, 40:885–895.

- [44] Welsh, C. J., Steelman, A. J., Mi, W., Young, C. R., Storts, R., Welsh, T. H., and Meagher, M. W. (2009). Neuroimmune interactions in a model of multiple sclerosis. *Annals of the New York Academy of Science*, 1153:209–219.
- [45] Wheeler, B. C. (2011). Introducing tbme letters special issue on multiscale modeling and analysis in computational biology and medicine: Part-1. *IEEE Transactions on Biomedical Engineering*, 58:2935.
- [46] Wiercigroch, M., and Budak, E. (2001). Sources of nonlinearities, chatter generation and suppression in metal cutting. *Philosophical Transactions of the Royal Society of London, A*, 359:663–693.
- [47] Young, J. Z. (1971). *The anatomy of the nervous system of Octopus vulgaris*. Oxford: Clarendon Press.